



This is a repository copy of *Genome-wide screen of cell-cycle regulators in normal and tumor cells identifies a differential response to nucleosome depletion.*

White Rose Research Online URL for this paper:
<https://eprints.whiterose.ac.uk/177426/>

Version: Published Version

Article:

Sokolova, M., Turunen, M., Mortusewicz, O. et al. (7 more authors) (2017) Genome-wide screen of cell-cycle regulators in normal and tumor cells identifies a differential response to nucleosome depletion. *Cell Cycle*, 16 (2). pp. 189-199. ISSN 1538-4101

<https://doi.org/10.1080/15384101.2016.1261765>

Reuse

This article is distributed under the terms of the Creative Commons Attribution (CC BY) licence. This licence allows you to distribute, remix, tweak, and build upon the work, even commercially, as long as you credit the authors for the original work. More information and the full terms of the licence here:
<https://creativecommons.org/licenses/>

Takedown

If you consider content in White Rose Research Online to be in breach of UK law, please notify us by emailing eprints@whiterose.ac.uk including the URL of the record and the reason for the withdrawal request.






eprints@whiterose.ac.uk
<https://eprints.whiterose.ac.uk/>

REPORT

 OPEN ACCESS

Genome-wide screen of cell-cycle regulators in normal and tumor cells identifies a differential response to nucleosome depletion

Maria Sokolova^a, Mikko Turunen^a, Oliver Mortusewicz^b, Teemu Kivioja ^a, Patrick Herr ^b, Anna Vähärautio ^a, Mikael Björklund^a, Minna Taipale^c, Thomas Helleday^b, and Jussi Taipale^{a,c}

^aGenome-Scale Biology Program, University of Helsinki, Helsinki, Finland; ^bScience for Life laboratory, Division of Translational Medicine and Chemical Biology, Department of Medical Biochemistry and Biophysics, Karolinska Institutet, Stockholm, Sweden; ^cDepartment of Medical Biochemistry and Biophysics, Karolinska Institutet, Stockholm, Sweden

ABSTRACT

To identify cell cycle regulators that enable cancer cells to replicate DNA and divide in an unrestricted manner, we performed a parallel genome-wide RNAi screen in normal and cancer cell lines. In addition to many shared regulators, we found that tumor and normal cells are differentially sensitive to loss of the histone genes transcriptional regulator CASP8AP2. In cancer cells, loss of CASP8AP2 leads to a failure to synthesize sufficient amount of histones in the S-phase of the cell cycle, resulting in slowing of individual replication forks. Despite this, DNA replication fails to arrest, and tumor cells progress in an elongated S-phase that lasts several days, finally resulting in death of most of the affected cells. In contrast, depletion of CASP8AP2 in normal cells triggers a response that arrests viable cells in S-phase. The arrest is dependent on p53, and preceded by accumulation of markers of DNA damage, indicating that nucleosome depletion is sensed in normal cells via a DNA-damage-like response that is defective in tumor cells.

ARTICLE HISTORY

Received 6 July 2016
Revised 21 October 2016
Accepted 11 November 2016

KEYWORDS

cancer; cell cycle; chromatin; DNA replication; functional genomics; nucleosome assembly; p53; RNA interference

Introduction

The cell cycle can be divided into two distinct periods, the interphase and the mitotic phase (M). During the interphase, cells are growing and duplicating their DNA, whereas in the mitotic phase, cells divide into two daughter cells. Interphase consists of three separate phases: gap1 (G1), DNA-synthesis (S) and gap2 (G2). Passing from one phase of cell cycle to the next is mainly regulated by cyclins and cyclin-dependent kinases. During the cell cycle, several checkpoints control that cells are ready to pass from one phase to the next. Interphase has two main checkpoints. One is in G1 phase, ensuring that everything is ready for DNA replication and the other is in G2 phase to verify that DNA replication is completed and that any damage to DNA is repaired. In addition, during the S phase, when the entire genome is replicated several checkpoint pathways can be activated as a response to DNA damage or stalled replication forks.

DNA replication is tightly coordinated with chromatin assembly, which depends on the recycling of parental histones and deposition of newly synthesized histones.¹ *Drosophila* and yeast *S. cerevisiae* cells can complete S phase without *de novo* histone synthesis.^{2,3} However, loss of histone expression or limiting assembly of nucleosomes to DNA by targeting chromatin assembly factors such as CAF-1, ASF1 and SLBP have been



reported to induce S phase arrest in human tumor cells.^{4–8} However, the mechanism of this arrest is still poorly understood.

Many regulators of the cell cycle have been identified by loss of function screens in yeast. Genome-wide RNAi screens have subsequently been used to identify both regulators that are conserved in and specific for higher organisms such as *Drosophila*⁹ and human.^{10–14} In addition to differences between species, regulation of the cell cycle is often altered in normal and tumor cells from the same organism. This is thought to be at least in part due to mutations in cell cycle regulatory proteins such as RB1¹⁵ and p53.¹⁶ However, a systematic comparative study that would identify regulators that are differentially required in normal and tumor cells has not been performed.


Results

Genome-wide RNAi screen identifies differential regulation of S-phase progression in normal and cancer cells

To understand similarities and differences in cell cycle regulation in normal and cancer cells, we performed a genome-wide RNAi screen simultaneously in two distinct cell lines: the osteosarcoma cell line U2OS and the hTERT-immortalized normal retinal pigment epithelial cell line hTERT-RPE1.

CONTACT Jussi Taipale  jussi.taipale@ki.se  Division of Functional Genomics and Systems Biology, Department of Medical Biochemistry and Biophysics, Karolinska Institutet, Scheeles Väg 2, SE-171 77 Stockholm, Sweden.

Color versions of one or more of the figures in the article can be found online at www.tandfonline.com/kccy.

 Supplemental data for this article can be accessed on the [publisher's website](#).

© 2017 Maria Sokolova, Mikko Turunen, Oliver Mortusewicz, Teemu Kivioja, Patrick Herr, Anna Vähärautio, Mikael Björklund, Minna Taipale, Thomas Helleday, and Jussi Taipale. Published with license by Taylor & Francis.

This is an Open Access article distributed under the terms of the Creative Commons Attribution License (<http://creativecommons.org/licenses/by/3.0/>), which permits unrestricted use, distribution, and reproduction in any medium, provided the original work is properly cited. The moral rights of the named author(s) have been asserted.

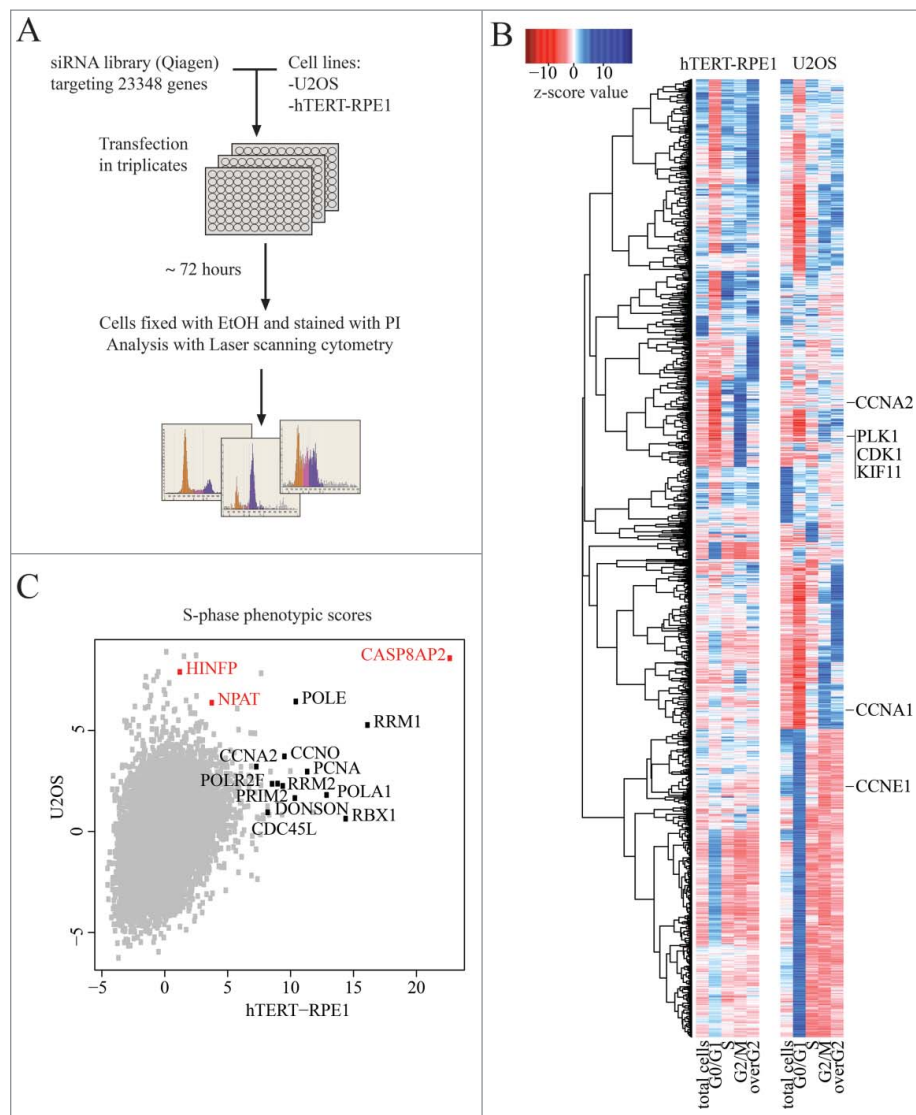


Figure 1. Genome-wide RNAi screen comparing normal and tumor cells. (A) Schematic representation of genome-scale RNAi screening in human immortalized (hTERT-RPE1) and cancer (U2OS) cell lines. (B) Hierarchical clustering of cell cycle regulators (z-score for at least one parameter is >5 or <-5) based on their phenotypic scores (for full data, see Supplementary Table S1). Note that known genes required for cell division (e.g., CDK1, KIF11, PLK1) cluster together for both cell lines. (C) S-phase z-scores in hTERT-RPE1 and U2OS cell lines. Most S-phase arrested hits for hTERT-RPE1 are genes involved in DNA replication and S-phase progression (marked black). Transcriptional regulators of histone genes are marked in red.

U2OS and hTERT-RPE1 cells grown on 96-well plates were transfected in triplicate with the same transfection mixes, containing pooled siRNAs (Qiagen) targeting a single gene per well. A total of 23 348 genes were targeted, and the cell cycle phase of the cells was analyzed after 3 d using laser scanning cytometry (Fig. 1A). For 17 095 targeted genes a total of 5 phenotypes were analyzed: the total number of cells, the fraction of cells in G1, S and G2 phases, and the fraction of cells that had higher DNA content than G2 phase cells (overG2; Fig. 1B, Table S1). These represent cells that have replicated DNA more than once without dividing.

In general, RNAi treatments targeting genes known to be required for mitosis (e.g. *CDK1*, *PLK1*, *KIF11*) had similar phenotypes in both cell lines (Fig. 1B, Fig. S1A). However, many genes whose loss decreased the fraction of cells in S-phase were different between the cell lines. Analysis of the hits using Gostat¹⁷ revealed that ribosomal proteins were enriched in this population in RPE1 cells (enriched GO terms: ribosome biogenesis (GO:0042254) p-value = 1.86e-

19, rRNA processing (GO:0006364) p-value = 2.9e-16, cytosolic ribosome (GO:0005830) p-value = 1.51e-10), whereas many ribosomal proteins and proteins involved in ribosome biogenesis (e.g., *WDR75*) caused an increase in S-phase of the U2OS tumor cells (Fig. S1B). This effect is likely due to the known role of p53 in detecting translational stress,^{18,19} and the weak activity of p53 pathway in U2OS cells due to MDM2 overexpression.²⁰ Consistently, in an earlier screen, Kittler et al. reported that in HeLa cells,¹⁴ which lack p53 function, loss of ribosomal proteins leads to increase in cells in S-phase.

Gostat analysis of the genes whose loss leads to an increase in S-phase also revealed that in hTERT-RPE1 cells, most of the S-phase arrested target genes (such as *PCNA*, *POLA1*, *RBX1*, *RRM2*) are required for DNA replication and DNA repair (enriched GO terms: DNA metabolic process (GO:0006259) p-value = 2.15e-06, cellular response to DNA damage stimulus (GO:0006974) p-value = 2.99e-06, DNA repair (GO:0006281) p-value = 5.54e-06) (Fig. 1C).

One of the strongest S-phase phenotypes in both cell lines was caused by siRNAs targeting caspase 8 associated protein 2 (*CASP8AP2*, also known as *FLASH*; Fig. 1C). *CASP8AP2* was originally identified as a caspase-8-associated protein,²¹ and is localized in several sub-nuclear bodies (promyelocytic leukemia bodies (PML bodies), Cajal bodies (CBs), and histone locus body (HLB)²²⁻²⁵) and has been reported to participate in several cellular processes, including processing of histone mRNAs,²⁶ regulation of apoptosis,^{21,27} and transcriptional control.²⁸⁻³⁰ *CASP8AP2* was also the strongest S-phase regulator in a secondary screen with a Dharmacon siRNA library targeting 55 of the identified cell cycle genes in nine different cell lines (Table S2, Fig. S2A). siRNA targeting of two other known regulators of histone gene transcription, *NPAT* and *HINFP* also resulted in an increase in the fraction of cells in the S-phase in most of the nine cell lines studied.

Loss of histone gene transcription regulators differentially affects S-phase progression

To validate disruption of S-phase progression by loss of the regulators of histone genes we transfected U2OS and hTERT-RPE1 cells with *CASP8AP2*, *NPAT*, *HINFP* and control siRNA pools (Fig. S2B) and then measured the DNA synthesis rate by incorporation of the thymidine analog 5-Ethynyl-2'-deoxyuridine (EdU). In both U2OS and hTERT-RPE1 cells, knockdown of *CASP8AP2* dramatically decreased EdU incorporation in S-phase. Knockdown of *NPAT* and *HINFP* had a similar effect in U2OS cells with accumulation of cells with poor EdU incorporation. However, in hTERT-RPE1 cells depletion of *NPAT* and *HINFP* failed to appreciably affect S-phase progression (Fig. 2A).

***CASP8AP2*, *NPAT*, *HINFP* and *E2F1* have different impact on histone gene expression**

To determine the effect of loss of *CASP8AP2*, *NPAT* and *HINFP* on histone gene expression, we profiled gene-expression in siRNA treated U2OS and hTERT-RPE1 cells using Affymetrix WT1.1 arrays (Table S3). We found that *CASP8AP2*, *NPAT* and *HINFP* do not regulate expression of each other, but mainly affect the expression of histone genes. Most histone genes were downregulated in U2OS cells following loss of *CASP8AP2*, *NPAT* or *HINFP* (Fig. 2B, Table S3). In normal cells, some highly expressed histone genes were downregulated (e.g., histone H3), albeit less than in tumor cells (Fig. S3). In addition, many histone genes that are normally expressed at lower levels were upregulated (Fig. S3).

To identify whether *CASP8AP2*, *NPAT* and *HINFP* directly bind to the histone gene promoter regions we performed ChIP-Seq in U2OS and hTERT-RPE1 cells. Consistent with previous findings, *HINFP* was found enriched near transcription start sites (TSSs) of replication-dependent histones H4 and H2B³¹⁻³⁴ (Tables S4 and S5). We also found that *HINFP* regulated two replication-independent histone H1 genes, H1F0 and H1FX (Tables S4 and S5). In contrast, *CASP8AP2* and *NPAT* ChIP-Seq peaks were only found colocalized at replication-dependent histone genes on chromosomes 1, 6 and 12 in both cell lines (Fig. 2C, Tables S4 and S5). These results indicate that *CASP8AP2* and *NPAT* regulate only replication-dependent histones, whereas *HINFP* regulates a subset of replication dependent histones (H4 and H2B), and two replication-independent H1 variants (H1F0 and H1FX).

Another histone gene regulator, *E2F1*,^{35,36} also bound to TSSs of many histone genes, including both replication dependent and independent histones (Tables S4 and S5). In addition, *E2F1* bound to the promoter of *CASP8AP2*, suggesting that *E2F* proteins control *CASP8AP2* and histone expression directly and via a feed-forward loop, respectively.

***CASP8AP2* knockdown results in low histone H3 protein levels and slows progression of replication forks in U2OS osteosarcoma cells**

To analyze the long-term effect of *CASP8AP2* loss on S-phase progression and histone protein levels, we treated U2OS and hTERT-RPE1 cells with *CASP8AP2* siRNAs, and analyzed DNA content, histone H3 protein level, and EdU incorporation by flow cytometry in the same population of the cells. We found that *CASP8AP2* siRNA treatment did not completely arrest U2OS cells in S-phase, but instead dramatically slowed down S-phase progression. The slow rate of EdU incorporation of S-phase cells at all time points analyzed, together with the moving of the S phase population to progressively higher DNA content over time indicates that the cells are progressing in S-phase at a very slow rate, with a single S-phase lasting more than 3 d on average (Fig. 3A).

The slowdown in S-phase was accompanied by increased cell death in U2OS, based on decrease in cell number over time, and increase in sub-G1 population in flow cytometry (Fig. S4B). In addition, we detected a marked decrease in histone H3 protein levels in the surviving cells that continued to replicate (Fig. 3B). In contrast, viable hTERT-RPE1 cells were arrested in early S-phase by *CASP8AP2* siRNA, and displayed also a decrease in histone H3 protein at this cell cycle stage. However, H3 protein levels appeared normal in cells that had progressed further in S-phase and in G2 cells (Fig. 3C-D). Analysis of total H3 protein level by western blot indicated that H3 levels were decreased in U2OS, but not in RPE1 cells (Fig. S4C). Control experiments established that as previously reported,³⁷ the vast majority of histone H3 protein in both cell lines is assembled to chromatin, indicating that very little free H3 exists in either cell type (Fig. S4D). This result indicates that U2OS cells can replicate their DNA in the absence of normal nucleosome levels, leading to accumulation of cells with low levels of H3. However, normal cells sense the depletion of the nucleosome pool and only complete DNA replication in the presence of sufficient amount of nucleosomes.

To identify the mechanism of the slowdown of the cell cycle in the U2OS cells, we analyzed the speed of replication forks in *CASP8AP2* siRNA treated U2OS cells using a DNA fiber assay, where DNA is labeled by two different labels consecutively, and then analyzed visually to detect the length of the labeled regions. This analysis confirmed earlier observations³⁸ that *CASP8AP2* siRNA generally decreases the speed by which replication forks progress (Fig. S5A-C), suggesting that in human cancer cells, individual replication forks are affected by nucleosomes loading behind them.

The ability of normal cells to activate H2AX phosphorylation in response to deregulation of histone expression is p53 dependent

To determine why normal and tumor cells respond differently to *CASP8AP2* loss, we examined the expression

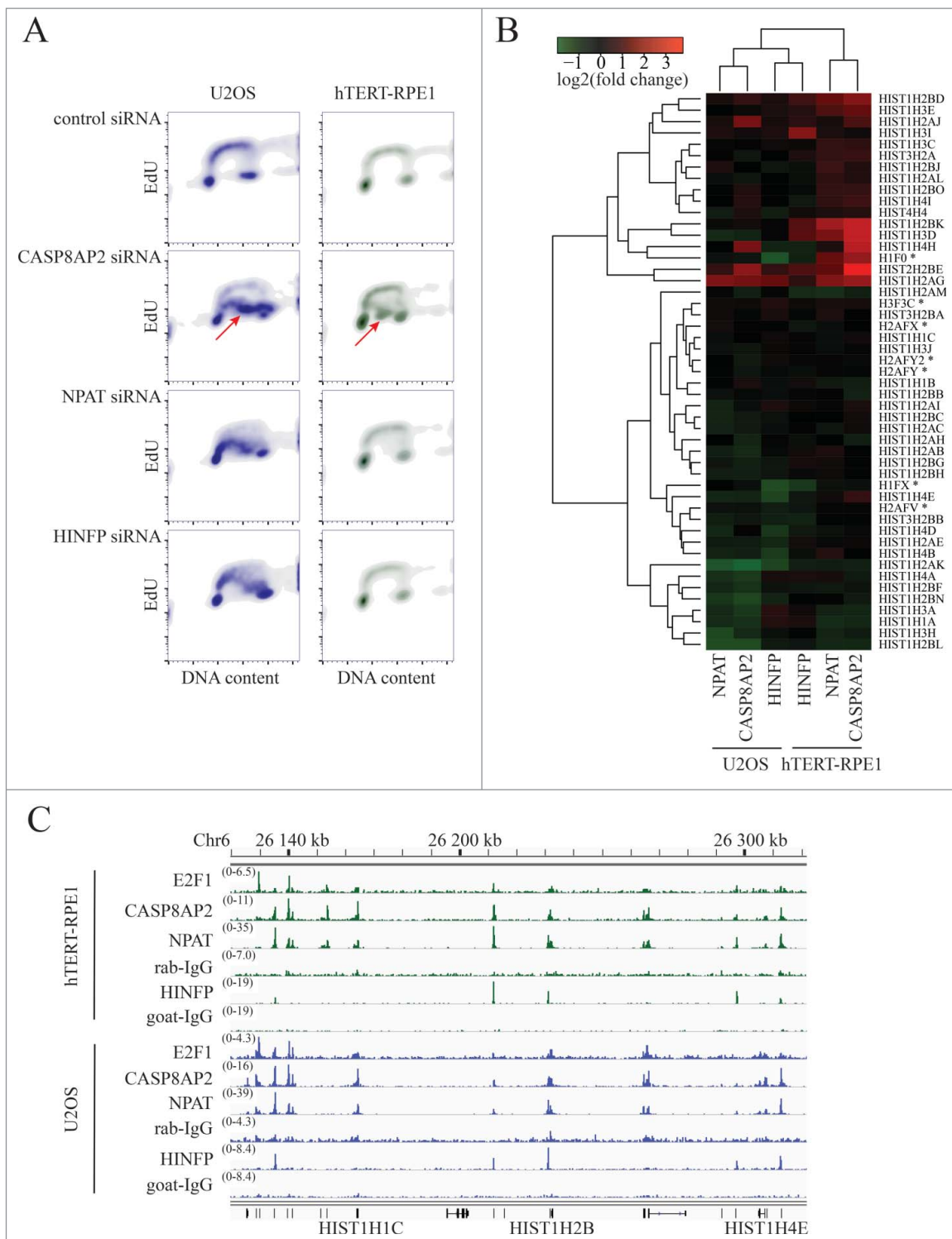


Figure 2. Regulation of DNA synthesis and expression of histone genes by CASP8AP2, NPAT and HINFP. (A) Flow cytometric analysis of DNA content (x-axis) and DNA replication (EdU incorporation; y-axis) shows partial or complete DNA synthesis progression 3 d after knockdown of CASP8AP2, NPAT and HINFP in tumor (U2OS) and normal (hTERT-RPE1) cells. Note that in both cell lines, CASP8AP2 RNAi results in formation of a population of S-phase cells with low EdU incorporation (red arrowheads). (B) Analysis of expression of histone genes following knockdown of the indicated genes in U2OS and hTERT-RPE1 cells. Replication-independent histone genes are marked with an asterisk. (C) Location-analysis of transcriptional regulators at histone gene cluster on chromosome 6p22. Cell lines and antibodies used in ChIP-Seq are indicated on the left, and signal intensity as number of reads is shown in parentheses above each track. Note that CASP8AP2 and NPAT co-bind to transcription start sites of replication-dependent histone genes (indicated in bottom) in this cluster.

profiles of non-histone genes after CASP8AP2, NPAT and HINFP siRNA treatment. This analysis revealed that p53 target genes were upregulated in hTERT-RPE1, but not in p53-proficient U2OS cells (Fig. 4A). The p53 target genes were upregulated relatively late, clearly after the changes in

histone gene expression were observed (Fig. S6A-B, Table S6).

One possibility that would explain the activation of p53 is that the slow replication causes DNA damage or a DNA damage-like state that is sensed by p53. Consistently with

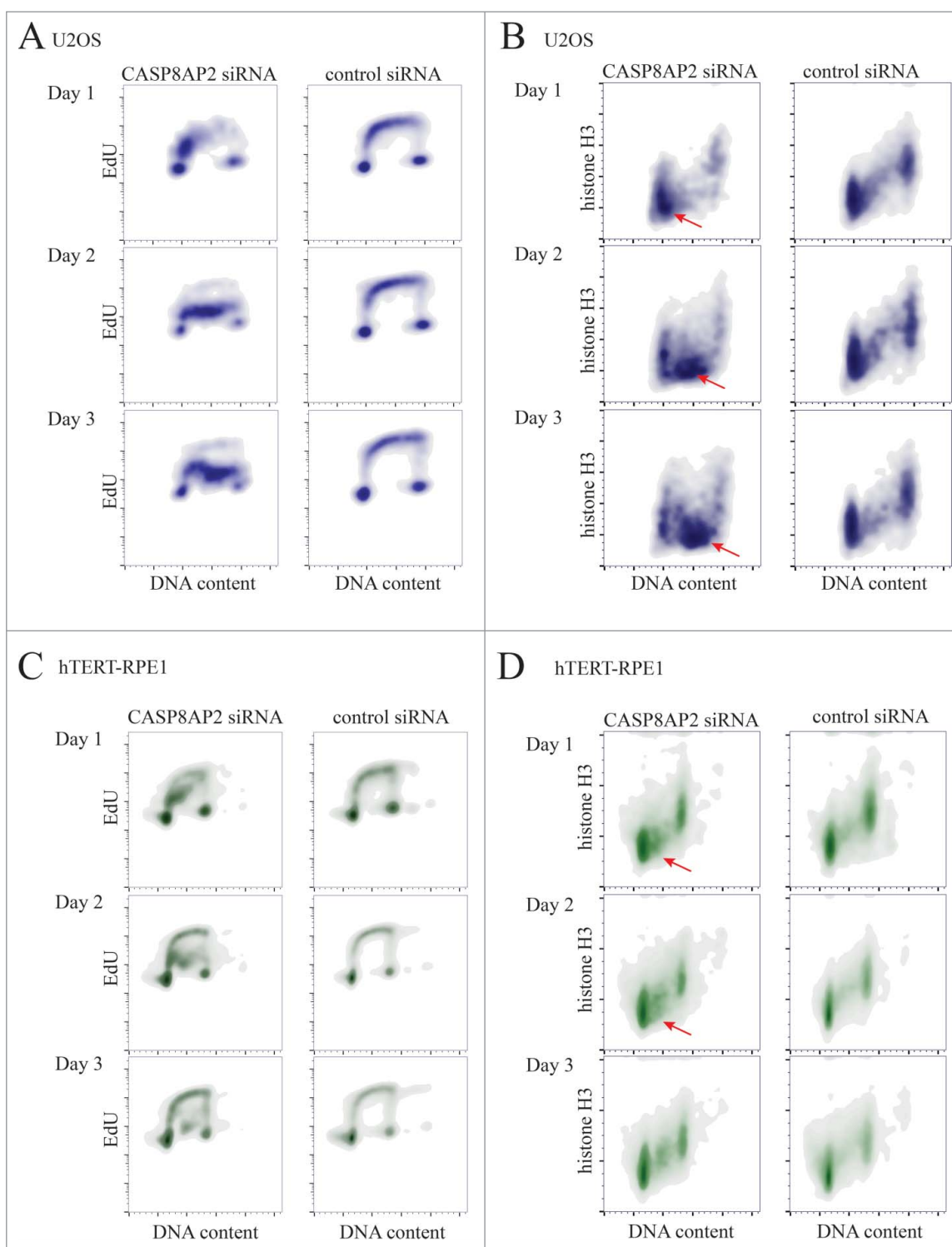


Figure 3. Tumor cells continue to progress in S-phase despite low nucleosome levels induced by CASP8AP2 knockdown. (A, B) Flow cytometry analysis of DNA content, DNA replication and histone H3 levels in siRNA treated cells. Note that tumor cells continue to replicate their DNA slowly (A) for multiple days, despite low amount of histone H3 (red arrowheads) (B). (C, D) Flow cytometry analysis of DNA content, DNA replication (EdU staining) and histone H3 levels in siRNA treated hTERT-RPE1 cells. Note that normal cells arrest in S-phase (C), and show decrease in histone H3 levels in early S-phase (red arrowheads) (D).

this hypothesis, an increase in a marker commonly associated with DNA damage, gamma-H2AX, was observed more in hTERT-RPE1 cell line (Fig. 4B, Fig. S6C-D) and less in U2OS cell line (Fig. 4C, Fig. S6C-D). We analyzed also other markers, which revealed modest increase in single-stranded DNA (RPA) and DNA damage repair (53BP1) markers, indicating that there is some DNA damage-like pathway activation also in U2OS cells,

but that this level of activation is not sufficient to completely arrest the cells in the S phase (Fig. S7A-D). To address whether the p53-dependent pathway is responsible for the S-phase arrest observed in normal but not in tumor cells, we analyzed the expression of the p53 target gene p21. We found that after CASP8AP2 RNAi treatment, p21 protein was induced more in hTERT-RPE1 cells (Fig. S8A), and only in S-phase cells that express elevated gamma-

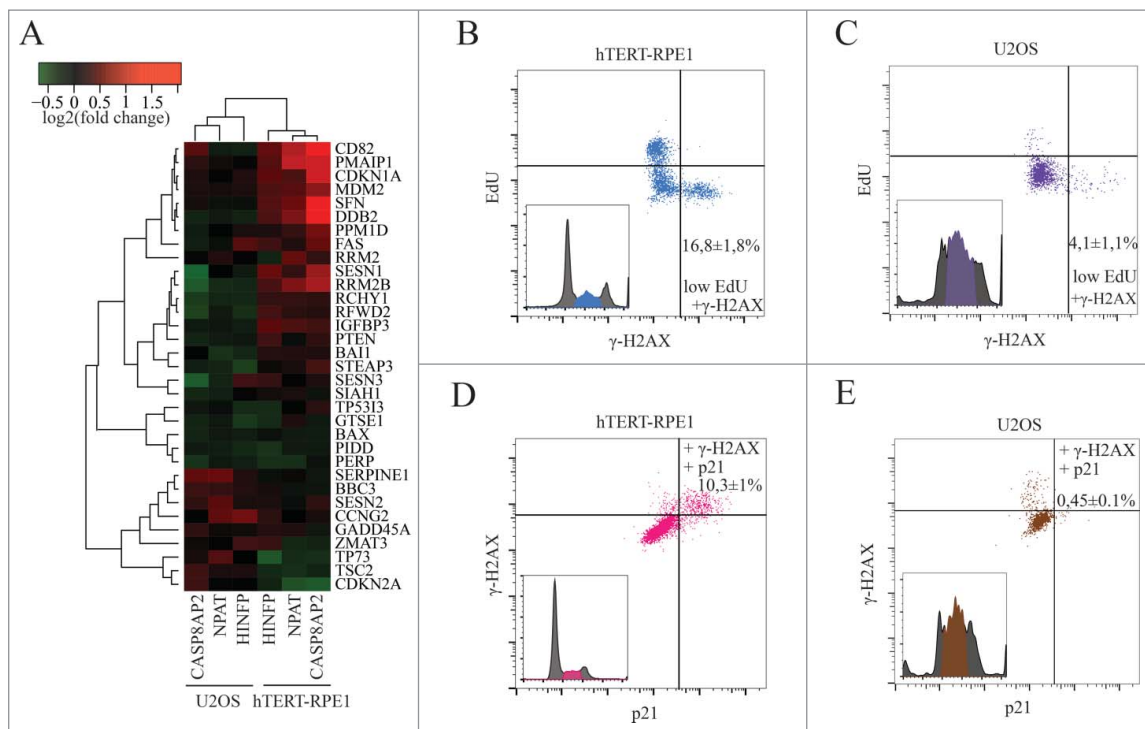


Figure 4. CASP8AP2 siRNA triggers activation of a p53 dependent S-phase checkpoint in normal but not in tumor cells. (A) Analysis of p53 target gene expression 3 d after knockdown of the indicated transcriptional regulators of histone genes. (B, C) Flow cytometry analysis of CASP8AP2 siRNA treated hTERT-RPE1 (B) and U2OS (C) cells indicates that non-replicated cells arrested in S-phase express a marker for DNA damage signaling (γ -H2AX; low right hand corner). (D, E) hTERT-RPE1 (D) but not U2OS (E) cells with activated DNA damage signaling have activated p53, based on expression of the p53 target-gene p21 (upper right hand corner).

H2AX (Fig. 4D–E). Similar results were found in two other normal human cell lines, HFL1 and CCD-1112Sk (Fig. S9A–D).

To test if the effect is dependent on p53, we generated a derivative of hTERT-RPE1 cell line that lacks p53 using CRISPR/Cas9 genome engineering. This cell line failed to completely arrest in S-phase or induce p21 in response to CASP8AP2 RNAi (Fig. S8A–B). In addition, significantly lower levels of gamma-H2AX accumulation were observed in the p53 deficient cell line (Figs. S6C–D and S9A–D). The response of the p53 deficient cell line was similar to that of tumor cells, including U2OS and HCT116 (Fig. S9A–D, Table S7).

Discussion

Genome-wide RNAi screens have become very powerful and informative approaches for the analysis of cell cycle regulation and for identification of new regulators of cell cycle progression and checkpoint control. Unlike previously published genome-wide RNAi screens performed to identify genes affecting cell cycle and cell size in *Drosophila* cells⁹ and in human cancer cells^{10–14} the present study compares two distinct cell lines: the osteosarcoma cell line U2OS and the hTERT-immortalized normal retinal pigment epithelial cell line hTERT-RPE1. As expected, several known mitotic regulators, and the known transcriptional regulator of histones, CASP8AP2 displayed strong phenotypes in both types of cells. However, some DNA-replication regulators, including two other transcriptional regulators of histones, HINFP and NPAT, displayed differential effects in the two cell types.

The canonical histones are exclusively expressed in S phase of cell cycle.^{36,39,40} This process is regulated by E2F and cyclin E-

Cdk2 kinase through phosphorylation of NPAT.^{33,35,41–43} Based on microarray data and flow cytometry, the depletion of CASP8AP2 caused strong downregulation of replication-dependent histones in U2OS cells. In normal cells, loss of CASP8AP2 also resulted in deregulation of histone expression, resulting in both positive and negative effects at the level of individual histone genes. The transcriptional regulation of histone genes by CASP8AP2 and NPAT is likely direct, based on their known interaction,⁴⁴ and our chromatin immunoprecipitation followed by sequencing (ChIP-seq) results showing localization of NPAT and CASP8AP2 almost exclusively to the replication-dependent histone loci.

In order to understand the mechanism behind the differential response of normal and tumor cells, we analyzed the S-phase phenotypes in more detail, using EdU incorporation assays in multiple tumor and normal cells depleted of CASP8AP2. This analysis revealed that the increase in cells in the S-phase observed in tumor cells after CASP8AP2 loss was not caused by an S-phase arrest. Instead, it resulted from a dramatic slowdown of DNA replication. In contrast, the S-phase progression of normal cells was arrested. Further analysis revealed also that the deregulation of nucleosome gene expression triggers a p53-dependent pathway in normal cells, but not in U2OS tumor cells. Thus, p53 activation is a consequence, not the cause, of the observed DNA replication phenotype.

One possibility that would explain the activation of p53 is that imbalance of histone proteins and the disruption of replication process causes DNA damage or a DNA damage-like state that is sensed by p53. Consistently with this hypothesis, an increase in a marker commonly associated with DNA damage, gamma-H2AX, was observed in hTERT-RPE1 cells following CASP8AP2 knockdown. Much lower levels of the marker

were seen in similarly treated U2OS cells. Thus, downregulation of histones in tested cancer cells could cause slow progression through S-phase without sufficient accumulation of DNA damage marker to activate p53-dependent cell cycle arrest. It is consistent with previous result where short-term depletion of histone genes by CASP8AP2 knockdown did not induce DNA damage markers.³⁸

In summary, we have through a genome-wide analysis of normal and tumor cells identified a significant difference in regulation of cell cycle arrest in response to abnormal regulation of histone genes transcription. In both normal and tumor cells, the depletion of CASP8AP2 alters mainly the expression of replication-dependent histones. Whereas hTERT-RPE1 cells respond by triggering a p53-dependent checkpoint, which leads to cell cycle arrest and recovery, U2OS cells continue to progress in S-phase, leading to cell death. The difference between normal and tumor cells was observed in all tested cell types, including eight tumor cell lines and three different normal cell types. Further investigation is necessary to assess the generality of this difference, and to determine whether the cell death in the cell lines studied here is caused by accumulation of DNA damage, or mediated more directly by CASP8AP2, which has been reported to have an anti-apoptotic role.²⁷ The identified defect in sensing histone expression levels could also in part explain the abnormal nuclear morphology commonly associated with cancer cells. Furthermore, the identified novel vulnerability of cancer cells can potentially be used for therapeutic purposes in the future.

Methods

Cell culture

U2OS human osteosarcoma (from M. Laiho lab, University Helsinki), HeLa human cervix adenocarcinoma (from M. Laiho lab, University Helsinki), HT1080 human fibrosarcoma (from ATCC, CRL-121), PC3 prostate adenocarcinoma (from Gonghong Wei, University Oulu), SK-N-MC human brain neuroepithelioma (from Gonghong Wei, University Oulu), SW480 colorectal adenocarcinoma (from Gonghong Wei, University Oulu) cells were cultured in DMEM supplemented with 10% fetal bovine serum and antibiotics (100 units/ml penicillin and 100 μ g/ml streptomycin). The hTERT-immortalized retinal pigment epithelial hTERT-RPE1 (from ATCC, CRL-4000) and hTERT-RPE1 p53KO cells lines were cultured in F12:DMEM(1:1) supplemented with 10% fetal bovine serum and antibiotics (100 units/ml penicillin, 100 μ g/ml streptomycin and 10 μ g/ml hygromycin B). SAOS-2 human osteosarcoma (from M. Laiho lab, University Helsinki) were cultured in McCoy's 5A medium supplemented with 10% fetal bovine serum and antibiotics (100 units/ml penicillin and 100 μ g/ml streptomycin). SJCRH30 human rhabdomyosarcoma cells (from ATCC, CRL-2061) were cultured in RPMI-1640 supplemented with 10% fetal bovine serum and antibiotics (100 units/ml penicillin and 100 μ g/ml streptomycin).

Chromatin immunoprecipitation followed by sequencing (ChIP-seq)

ChIP assays were performed as previously described.⁴⁵ Immunoprecipitations were performed with 5 μ g antibody against

CASP8AP2 (sc-9088, Santa Cruz Biotechnology), NPAT (sc-67007, Santa Cruz Biotechnology), HINFP (sc-49818, Santa Cruz Biotechnology), E2F1 (sc-193, Santa Cruz Biotechnology), normal rabbit IgG (sc-2027, Santa Cruz Biotechnology) and normal goat IgG (sc-2028, Santa Cruz Biotechnology).

ChIP libraries were prepared for Illumina Genome Analyzer or HiSeq2000 sequencing as described before.⁴⁵ Sequencing reads were mapped to the human genome (NCBI36) and peaks called as described.⁴⁶ Lists of all significant peaks ($p > 0.00001$, fold change > 2) are in Supplementary Table S4.

Laser scanning cytometry: Genome-wide RNAi screen

A Qiagen Human Whole Genome siRNA Set V4.0 was used for transfection in U2OS and hTERT-RPE1 cell lines. Qiagen siRNA library contains 4 pooled siRNAs in total amount of 0.5 nmol siRNA per well targeting 23348 different genes (EntrezGene ID). The complete set contains a total of 308×96 -well plates with each plate containing 80 wells with siRNA constructs as well as following controls: Qiagen negative control siRNA, siRNA against GFP (Qiagen), 3 wells with transfection reagent and 3 wells with siRNA against CDK1 (custom made positive control purchased from MWG).

For reverse transfection 4000 cells were plated in the growth medium into 96-well plates having 15 nM siRNA and 0.7 μ l HiPerFect (Qiagen) in total volume of 125 μ l. Transfection was performed in triplicates simultaneously for U2OS and hTERT-RPE1 cells in 16 batches. After 70–72 hours of incubation cells were washed with PBS, fixed with 70% ice cold ethanol o/n and stained with PBS containing 30 μ g/ml PI (Sigma-Aldrich) and 30 μ g/ml RNase A (MACHEREY-NAGEL). The stained cells were scanned with an Acumen eX3 microplate cytometer (TTP LabTech).

The number of the cells in each sub-population of the cell cycle was calculated with Acumen eX3 software. Single cell population was specified based on area, depth and width parameters of the signal for each object. The DNA content histograms were gated manually for each batch to specify sub-G1-, G0/G1-, S-, G2/M- and over- G2-phase populations. Total cell number and percentages of the cells in each population were normalized two times: first using median of a plate and then median of the well position in all plates (positive controls were excluded from the normalization); then Z-score were calculated for each parameter from the median of triplicates and median of all negative controls (i.e. negative control siRNA and GFP siRNA): $Z = (x - \mu) / \sigma$, where x is the median of triplicates for each parameter; μ is the median of all negative controls; σ is the standard deviation of all negative controls.

For the final data analysis, the siRNA sequences were mapped to human transcripts (Ensembl version 52, genome assembly NCBI36) using bowtie version 0.11.3. In total 79534 (81.36%) siRNAs were mapped to at least one transcript without mismatches and 17095 (73%) wells have 4 siRNAs mapping the same single target gene. After normalization only data from the 17095 samples were used for further analysis. To identify hits ± 5 z-score cutoff was applied for all calculated parameters (sub-G1, G0/G1, S, G2/M and over-G2), later on subG1 was excluded from the analysis as non-informative.

Data analysis and visualization was performed in R using *hopach* (R package version 2.20.0; <http://www.stat.berkeley.edu/~laan/>, <http://docpollard.org/>),⁴⁷ *gplots* packages and *GStat*(<http://gostat.wehi.edu.au/>).¹⁷

Secondary screen

A Dharmacon siGENOME SMARTpool of 91 siRNAs (including negative controls) was used for transfection in 9 different cells lines (hTERT-RPE1, U2OS, SAOS-2, SJCRH30, HeLa, PC3, SK-N-MC, SW480 and HT1080). Transfection, screening and data analysis was performed in the same way as with the Qiagen library screen.

Microarray data

Sets of 4 FlexiTube GeneSolution siRNAs (Qiagen) targeting CASP8AP2, NPAT, HINFP or AllStars Negative Control (Qiagen) were used. For reverse transfection protocol, cells at 30% confluence were plated in the growth medium into 6-well plates using 15 nM siRNA and 7 μ l HiPerFect (Qiagen) in final total volume 2.1 ml. Transfection was performed in duplicates simultaneously for each siRNA for U2OS and hTERT-RPE1 cell lines. After 70–72 hours growing cells were collected and RNA extraction was performed with RNeasy kit (Qiagen) including DNase treatment according to manufacturer's protocol. RNA was analyzed using Affymetrix Human WT 1.1 arrays in the core facility for Bioinformatics and Expression Analysis (Karolinska Institute, Stockholm, Sweden). Raw CEL data were analyzed using the Bioconductor R packages *affy*⁴⁸ and *limma*⁴⁹ and for the annotation custom CDF files (ENSG)⁵⁰ was used. p53 pathway data was retrieved from KEGG (<http://www.genome.jp/kegg/>).

Flow cytometry

Sets of 4 FlexiTube GeneSolution siRNAs (Qiagen) against CASP8AP2, NPAT, HINFP or AllStars Negative Control (Qiagen) were used for reverse transfection protocol as in microarray analysis. Although the replicates performed in the same day are highly consistent, and qualitatively similar phenotypes were reproducibly observed in experiments performed in different days, some variance to the penetrance of the phenotypes was observed between experiments performed in different days (e.g., Supplementary Fig S8 and Fig. 4). This effect does not materially affect the conclusions drawn, and is most likely attributable to differences in transfection efficiency.

Cells were incubated with 10 μ M EdU (Life Technologies) for last 1 hour before harvesting and fixing with 70% ice cold ethanol on 1, 2 and 3 d after transfection. The cells were washed with 1% BSA in PBS and prepared for flow cytometry with Click-iT[®] EdU Alexa Fluor[®] 647 Flow Cytometry Assay Kit (Life Technologies) according to the manufacturer's protocol.

For the flow cytometry analysis of total histone H3 cells were harvested and fixed with 70% ice cold ethanol on 1, 2 and 3 d after transfection and left overnight in -20°C . On the next day the cells were washed with 1% BSA in PBS several times and blocked in 1% BSA in PBS for at least an hour followed by overnight incubation at $+4^{\circ}\text{C}$ with

histone H3 antibody (1:500, #9715, Cell Signaling Technology, or 1:500, ab1791, Abcam), γ -H2AX(1:500, #9718, Cell Signaling Technology), p21 (1:100, sc-6246, Santa Cruz Biotechnology) or as a control normal rabbit IgG (1:200, sc-3888, Santa Cruz Biotechnology), normal mouse IgG (1:200, sc-2025, Santa Cruz Biotechnology). The cells were washed several times with 1% BSA in PBS and incubated with secondary antibodies (anti-rabbit Alexa488 or anti-mouse Alexa488, Life Technologies) for an hour. After several washes with 1% BSA in PBS cells were stained for DNA content with 5 μ M DRAQ5 (BioStatus Limited) and 10 mg/ml RNaseA (MACHEREY-NAGEL) for 30 min. Flow cytometry was performed using MACSQuant Analyzer (Miltenyi Biotec) and data analyzed using FlowJo (FlowJo, LLC).

Western blotting analysis

Different subcellular protein fractions from hTERT-RPE1 and U2OS cells were extracted using Subcellular Protein Fractionation Kit for Cultured Cells (78840, Pierce Biotechnology) according to the manufacturer's protocol. Samples were prepared in Laemmli sample buffer and analyzed with 10%-SDS PAGE followed by immunoblotting analysis using the following antibodies: histone H3 (#9715, Cell Signaling Technology) and α -tubulin (T9026, Sigma-Aldrich).

For the total histone H3 level analysis sets of 4 FlexiTube GeneSolution siRNAs (Qiagen) against CASP8AP2 or AllStars Negative Control (Qiagen) were used for reverse transfection protocol in 6-well plates as described in microarray analysis. 10 μ g of total protein was analyzed by 10% SDS-PAGE followed by immunoblotting analysis using the following antibodies: histone H3 (#9715, Cell Signaling Technology) and α -tubulin (T9026, Sigma-Aldrich).

Detection of the antibodies was performed with Pierce ECL plus western blotting substrate (#32132, ThermoScientific) and processed with Gel Doc[™] XR+ and ChemiDoc[™] XRS+ Systems with Image Lab[™] 5.0 Software (Bio-Rad).

Genome editing

Generating hTERT-RPE1 p53KO cell line using CRISPR (clustered regularly interspaced short palindromic repeats) in complex with Cas9 (CRISPR associated protein 9) protein technology was performed according previously published protocol.⁵¹

The following two 23 bp guide RNAs (gRNAs) in the p53 coding region were designed using the CRISPR web tool (<http://crispr.mit.edu/>):

TP53_1 in exon 4: GCATTGTTCAATATCGTCCGGG

TP53_2 in exon 2: GCGACGCTAGGATCTGACTGCGG

Selected target sequences were incorporated into two 60-mer oligonucleotides corresponding the exon 4 and exon two targets.

TP53_1F for exon 4:

TTTCTTGCTTTTATATATCTTGTGGAAAGGACGAAACA
CCGCATTGTTCAATATCGTCCG

TP53_1R for exon 4:

GACTAGCCTTATTTAACTTGCTATTTCTAGCTCTA
AAACCGGACGATATTGAACAATGC

TP53_2F for exon 2:

TTTCTTGGCTTTATATATCTTGTGGAAAGGACGAAAC
ACCGCGACGCTAGGATCTGACTG

TP53_2R for exon 2:

GACTAGCCTTATTTTAACTTGCTATTTCTAGCTCTAA
AACCAGTCAGATCCTAGCGTCGC

The two oligos were annealed and extended for 30 min at 72°C to make a 100 bp double stranded DNA fragment using Phusion polymerase (NEB). Using Gibson assembly (NEB) reaction according to the manufacturer's protocol the 100 bp DNA fragments were incorporated into the gRNA cloning vector (<http://www.addgene.org/41824/>) and the reaction products were transformed into chemically competent DH5 α cells. Plasmid DNA from 5 single colonies for both constructs (TP53_1 and TP53_2) were extracted using Plasmid midiprep (Qiagen).

After sequence verification plasmids containing insertions with TP53_1 and TP53_2 gDNAs were co-transfected with hCas9 plasmid (<http://www.addgene.org/41815/>) into the hTERT-RPE1 cells using FuGENE[®] HD Transfection Reagent (Promega) according to the manufacturer's protocol.

To confirm genome editing 2 d after transfection cells were split and genotyped using Phusion polymerase (NEB) with following primers:

gDNA_p53_F: AACTGACAGGAAGCCAAAGGG

gDNA_p53_R: ATCCCCACTTTTCTCTTGCAGC

The cells with p53 KO phenotype were split in low density into several 96 well plates to obtain single-cell colonies. After several single-cell colonies had reached confluence they were split and p53 levels were verified with Western Blotting using p53 antibody (1:200, DO-1, sc-126, Santa Cruz Biotechnology) as described above. In three hTERT-RPE1 clones p53 protein was not detected and p53 status was verified with Sanger sequencing of genomic and cDNA with gDNA_p53 primers and cDNA primers:

cDNA_p53_F: CAGCCAGACTGCCTTCCG

cDNA_p53_R: GACAGGCACAAACACGCACC

Of the obtained clones, we chose to use a clone with a homozygous 1 bp insertion in exon 4 of p53, causing a frameshift mutation at codon position 48, resulting in mutation of Asp 48 to Glu, and truncation of the protein after two amino-acid out-of-frame peptide (Glu-Arg-Tyr-**Stop**).

DNA fiber assay

2 × 10⁵ U2OS cells were reverse transfected with either 15 nM control or CASP8AP2 siRNA according to the manufacturer's protocol (HiPerFect, Qiagen). After 48 h, cells were pulse labeled with 25 mM CldU followed by 250 mM IdU for 20 min each and harvested immediately. DNA fiber spreads were prepared as previously described.²⁹ In short, DNA was denatured using 2.5M HCl and incubated with rat anti-BrdU monoclonal antibody (AbD Serotec, 1:1000) and mouse monoclonal anti-BrdU antibody (Becton Dickinson, 1:750) overnight at 4°C. Objective slides were fixed in 4% formaldehyde and subsequently incubated with an AlexaFluor 555-conjugated goat anti-rat IgG and AlexaFluor 488-conjugated goat anti-mouse IgG (Molecular Probes, 1:500) for 1.5 h at room temperature. Stained DNA fibers were imaged with a Zeiss LSM710 confocal laser scanning microscope, equipped with a Plan-Apochromat

63x/1.40 Oil DIC M27 objective. Alexa 488 and 555 were excited with a 488 nm Ar laser line and a 561 nm DPSS laser line, respectively. Confocal images were recorded with a frame size of 1024 × 1024 pixels and a pixel size of 130 nm. CldU and IdU track length were measured using ImageJ (<http://rsb.info.nih.gov/ij/>) and mm values were converted into kb using the conversion factor 1mm = 2.59 kb.⁵²

Primary array and sequencing data are deposited in the Gene Expression Omnibus (GEO) under accession number GSE69149.

Disclosure of potential conflicts of interest

No potential conflicts of interest were disclosed.

Acknowledgments

We thank Sini Miettinen for technical assistance, Drs. M. Laiho and G. Wei for supplying several cell lines and Dr. Bernhard Schmierer for critical review of the manuscript.

Funding

This work was supported by the Academy of Finland Center of Excellence in Cancer Genetics and Finnish Cancer Organizations.

Author contributions

M.S. performed most of the experiments with help from M.Tur.

O.M. performed DNA fiber assay, P.H. performed immunofluorescence experiments. T.K. performed siRNA sequences mapping to human transcripts. M.S. performed data analyses and interpreted the results with input from M.B., M.T., T.K. and A.V.

T. H. and J.T. supervised experiments and data analysis. M.S and J.T. wrote the manuscript. M.S., M.Tur., T.K., A.V., M.B., M.T., T.H. and J.T. discussed the results and commented on the manuscript.

ORCID

Teemu Kivioja  <http://orcid.org/0000-0002-7732-2177>

Patrick Herr  <http://orcid.org/0000-0003-2945-966X>

Anna Vähärautio  <http://orcid.org/0000-0003-4721-3954>

References

- [1] Nelson DM, Ye X, Hall C, Santos H, Ma T, Kao GD, Yen TJ, Harper JW, Adams PD. Coupling of DNA synthesis and histone synthesis in S phase independent of cyclin/cdk2 activity. *Mol Cell Biol* 2002; 22:7459-72; PMID:12370293; <http://dx.doi.org/10.1128/MCB.22.21.7459-7472.2002>
- [2] Gunesdogan U, Jackle H, Herzig A. Histone supply regulates S phase timing and cell cycle progression. *eLife* 2014; 3:e02443; PMID:25205668; <http://dx.doi.org/10.7554/eLife.02443>
- [3] Kim UJ, Han M, Kayne P, Grunstein M. Effects of histone H4 depletion on the cell cycle and transcription of *Saccharomyces cerevisiae*. *EMBO J* 1988; 7:2211-9; PMID:3046933
- [4] Nabatiyan A, Krude T. Silencing of chromatin assembly factor 1 in human cells leads to cell death and loss of chromatin assembly during DNA synthesis. *Mol Cell Biol* 2004; 24:2853-62; PMID:15024074; <http://dx.doi.org/10.1128/MCB.24.7.2853-2862.2004>
- [5] Groth A, Corpet A, Cook AJ, Roche D, Bartek J, Lukas J, Almuzni G. Regulation of replication fork progression through histone supply and demand. *Science* 2007; 318:1928-31; PMID:18096807; <http://dx.doi.org/10.1126/science.1148992>

- [6] Ye X, Franco AA, Santos H, Nelson DM, Kaufman PD, Adams PD. Defective S phase chromatin assembly causes DNA damage, activation of the S phase checkpoint, and S phase arrest. *Mol Cell* 2003; 11:341-51; PMID:12620223; [http://dx.doi.org/10.1016/S1097-2765\(03\)00037-6](http://dx.doi.org/10.1016/S1097-2765(03)00037-6)
- [7] Hoek M, Stillman B. Chromatin assembly factor 1 is essential and couples chromatin assembly to DNA replication in vivo. *Proc Natl Acad Sci U S A* 2003; 100:12183-8; PMID:14519857; <http://dx.doi.org/10.1073/pnas.1635158100>
- [8] Sullivan KD, Mullen TE, Marzluff WF, Wagner EJ. Knockdown of SLBP results in nuclear retention of histone mRNA. *Rna* 2009; 15:459-72; PMID:19155325; <http://dx.doi.org/10.1261/rna.1205409>
- [9] Bjorklund M, Taipale M, Varjosalo M, Saharinen J, Lahdenpera J, Taipale J. Identification of pathways regulating cell size and cell-cycle progression by RNAi. *Nature* 2006; 439:1009-13; PMID:16496002; <http://dx.doi.org/10.1038/nature04469>
- [10] Mukherji M, Bell R, Supekova L, Wang Y, Orth AP, Batalov S, Miraglia L, Huesken D, Lange J, Martin C, et al. Genome-wide functional analysis of human cell-cycle regulators. *Proc Natl Acad Sci U S A* 2006; 103:14819-24; PMID:17001007; <http://dx.doi.org/10.1073/pnas.0604320103>
- [11] Kittler R, Surendranath V, Heninger AK, Slabicki M, Theis M, Putz G, Franke K, Caldarelli A, Grabner H, Kozak K, et al. Genome-wide resources of endoribonuclease-prepared short interfering RNAs for specific loss-of-function studies. *Nat Methods* 2007; 4:337-44; PMID:17351622
- [12] Fuchs F, Pau G, Kranz D, Sklyar O, Budjan C, Steinbrink S, Horn T, Pedal A, Huber W, Boutros M. Clustering phenotype populations by genome-wide RNAi and multiparametric imaging. *Mol Systems Biol* 2010; 6:370; PMID:20531400; <http://dx.doi.org/10.1038/msb.2010.25>
- [13] Neumann B, Walter T, Heriche JK, Bulkescher J, Erfle H, Conrad C, Rogers P, Poser I, Held M, Liebel U, et al. Phenotypic profiling of the human genome by time-lapse microscopy reveals cell division genes. *Nature* 2010; 464:721-7; PMID:20360735; <http://dx.doi.org/10.1038/nature08869>
- [14] Kittler R, Pelletier L, Heninger AK, Slabicki M, Theis M, Miroslaw L, Poser I, Lawo S, Grabner H, Kozak K, et al. Genome-scale RNAi profiling of cell division in human tissue culture cells. *Nat Cell Biol* 2007; 9:1401-12; PMID:17994010; <http://dx.doi.org/10.1038/ncb1659>
- [15] Manning AL, Dyson NJ. RB: mitotic implications of a tumour suppressor. *Nat Rev Cancer* 2012; 12:220-6; PMID:22318235
- [16] Vogelstein B, Lane D, Levine AJ. Surfing the p53 network. *Nature* 2000; 408:307-10; PMID:11099028; <http://dx.doi.org/10.1038/35042675>
- [17] Beißbarth T, Speed TP. Gostat: find statistically overrepresented Gene Ontologies within a group of genes. *Bioinformatics* 2004; 20:1464-5; <http://dx.doi.org/10.1093/bioinformatics/bth088>
- [18] Deisenroth C, Zhang Y. Ribosome biogenesis surveillance: probing the ribosomal protein-Mdm2-p53 pathway. *Oncogene* 2010; 29:4253-60; PMID:20498634; <http://dx.doi.org/10.1038/onc.2010.189>
- [19] Zhang Y, Lu H. Signaling to p53: ribosomal proteins find their way. *Cancer cell* 2009; 16:369-77; PMID:19878869; <http://dx.doi.org/10.1016/j.ccr.2009.09.024>
- [20] Florenes VA, Maelandsmo GM, Forus A, Andreassen A, Myklebost O, Fodstad O. MDM2 gene amplification and transcript levels in human sarcomas: relationship to TP53 gene status. *J Natl Cancer Inst* 1994; 86:1297-302; PMID:8064888; <http://dx.doi.org/10.1093/jnci/86.17.1297>
- [21] Imai Y, Kimura T, Murakami A, Yajima N, Sakamaki K, Yonehara S. The CED-4-homologous protein FLASH is involved in Fas-mediated activation of caspase-8 during apoptosis. *Nature* 1999; 398:777-85; PMID:10235259; <http://dx.doi.org/10.1038/19709>
- [22] Barcaroli D, Dinsdale D, Neale MH, Bongiorno-Borbone L, Ranalli M, Munarriz E, Sayan AE, McWilliam JM, Smith TM, Fava E, et al. FLASH is an essential component of Cajal bodies. *Proc Natl Acad Sci U S A* 2006; 103:14802-7; PMID:17003126; <http://dx.doi.org/10.1073/pnas.0604225103>
- [23] Milovic-Holm K, Kriehoff E, Jensen K, Will H, Hofmann TG. FLASH links the CD95 signaling pathway to the cell nucleus and nuclear bodies. *EMBO J* 2007; 26:391-401; PMID:17245429; <http://dx.doi.org/10.1038/sj.emboj.7601504>
- [24] Bongiorno-Borbone L, De Cola A, Vernole P, Finos L, Barcaroli D, Knight RA, Melino G, De Laurenzi V. FLASH and NPAT positive but not Coilin positive Cajal Bodies correlate with cell ploidy. *Cell cycle* 2008; 7:2357-67; PMID:18677100; <http://dx.doi.org/10.4161/cc.6344>
- [25] Vennemann A, Hofmann TG. SUMO regulates proteasome-dependent degradation of FLASH/Casp8AP2. *Cell cycle* 2013; 12:1914-21; PMID:23673342; <http://dx.doi.org/10.4161/cc.24943>
- [26] Yang XC, Burch BD, Yan Y, Marzluff WF, Dominski Z. FLASH, a proapoptotic protein involved in activation of caspase-8, is essential for 3' end processing of histone pre-mRNAs. *Mol Cell* 2009; 36:267-78; PMID:19854135; <http://dx.doi.org/10.1016/j.molcel.2009.08.016>
- [27] Chen S, Evans HG, Evans DR. FLASH knockdown sensitizes cells to Fas-mediated apoptosis via down-regulation of the anti-apoptotic proteins, MCL-1 and Cflip short. *PloS one* 2012; 7:e32971; PMID:22427918; <http://dx.doi.org/10.1371/journal.pone.0032971>
- [28] Alm-Kristiansen AH, Saether T, Matre V, Gilfillan S, Dahle O, Gabrielsen OS. FLASH acts as a co-activator of the transcription factor c-Myb and localizes to active RNA polymerase II foci. *Oncogene* 2008; 27:4644-56; PMID:18408764; <http://dx.doi.org/10.1038/onc.2008.105>
- [29] Kino T, Chrousos GP. Tumor necrosis factor alpha receptor- and Fas-associated FLASH inhibit transcriptional activity of the glucocorticoid receptor by binding to and interfering with its interaction with p160 type nuclear receptor coactivators. *J Biol Chem* 2003; 278:3023-9; PMID:12477726; <http://dx.doi.org/10.1074/jbc.M209234200>
- [30] Hummon AB, Pitt JJ, Camps J, Emons G, Skube SB, Huppi K, Jones TL, Beissbarth T, Kramer F, Grade M, et al. Systems-wide RNAi analysis of CASP8AP2/FLASH shows transcriptional deregulation of the replication-dependent histone genes and extensive effects on the transcriptome of colorectal cancer cells. *Molecular cancer* 2012; 11:1; PMID:22216762; <http://dx.doi.org/10.1186/1476-4598-11-1>
- [31] Mitra P, Xie RL, Medina R, Hovhannisyan H, Zaidi SK, Wei Y, Harper JW, Stein JL, van Wijnen AJ, Stein GS. Identification of HiNF-P, a key activator of cell cycle-controlled histone H4 genes at the onset of S phase. *Mol Cell Biol* 2003; 23:8110-23; PMID:14585971; <http://dx.doi.org/10.1128/MCB.23.22.8110-8123.2003>
- [32] Miele A, Braastad CD, Holmes WF, Mitra P, Medina R, Xie R, Zaidi SK, Ye X, Wei Y, Harper JW, et al. HiNF-P directly links the cyclin E/CDK2/p220NPAT pathway to histone H4 gene regulation at the G1/S phase cell cycle transition. *Mol Cell Biol* 2005; 25:6140-53; PMID:15988025; <http://dx.doi.org/10.1128/MCB.25.14.6140-6153.2005>
- [33] Zhao J, Kennedy BK, Lawrence BD, Barbie DA, Matera AG, Fletcher JA, Harlow E. NPAT links cyclin E-Cdk2 to the regulation of replication-dependent histone gene transcription. *Genes & development* 2000; 14:2283-97; PMID:10995386; <http://dx.doi.org/10.1101/gad.827700>
- [34] Barcaroli D, Bongiorno-Borbone L, Terrinoni A, Hofmann TG, Rossi M, Knight RA, Matera AG, Melino G, De Laurenzi V. FLASH is required for histone transcription and S-phase progression. *Proc Natl Acad Sci U S A* 2006; 103:14808-12; PMID:17003125; <http://dx.doi.org/10.1073/pnas.0604227103>
- [35] Gokhman D, Livyatan I, Sailaja BS, Melcer S, Meshorer E. Multilayered chromatin analysis reveals E2f, Smad and Zfx as transcriptional regulators of histones. *Nature structural & molecular biology* 2013; 20:119-26; PMID:23222641; <http://dx.doi.org/10.1038/nsmb.2448>
- [36] Grant GD, Brooks L, 3rd, Zhang X, Mahoney JM, Martyanov V, Wood TA, Sherlock G, Cheng C, Whitfield ML. Identification of cell cycle-regulated genes periodically expressed in U2OS cells and their regulation by FOXM1 and E2F transcription factors. *Molecular biology of the cell* 2013; 24:3634-50; PMID:24109597; <http://dx.doi.org/10.1091/mbc.E13-05-0264>
- [37] Jackson V. In vivo studies on the dynamics of histone-DNA interaction: evidence for nucleosome dissolution during replication and transcription and a low level of dissolution independent of both. *Biochemistry* 1990; 29:719-31; PMID:1692479; <http://dx.doi.org/10.1021/bi00455a019>
- [38] Meiljvang J, Feng Y, Alabert C, Neelsen KJ, Jasencakova Z, Zhao X, Lees M, Sandelin A, Pasero P, Lopes M, et al. New histone supply

- regulates replication fork speed and PCNA unloading. *The Journal of cell biology* 2014; 204:29-43; PMID:24379417; <http://dx.doi.org/10.1083/jcb.201305017>
- [39] Marzluff WF, Wagner EJ, Duronio RJ. Metabolism and regulation of canonical histone mRNAs: life without a poly(A) tail. *Nature reviews Genetics* 2008; 9:843-54; PMID:18927579; <http://dx.doi.org/10.1038/nrg2438>
- [40] Whitfield ML, Sherlock G, Saldanha AJ, Murray JI, Ball CA, Alexander KE, Matese JC, Perou CM, Hurt MM, Brown PO, et al. Identification of genes periodically expressed in the human cell cycle and their expression in tumors. *Molecular biology of the cell* 2002; 13:1977-2000; PMID:12058064; <http://dx.doi.org/10.1091/mbc.02-02-0030>
- [41] Zhao J, Dynlacht B, Imai T, Hori T, Harlow E. Expression of NPAT, a novel substrate of cyclin E-CDK2, promotes S-phase entry. *Genes & development* 1998; 12:456-61; PMID:9472014; <http://dx.doi.org/10.1101/gad.12.4.456>
- [42] Ma T, Van Tine BA, Wei Y, Garrett MD, Nelson D, Adams PD, Wang J, Qin J, Chow LT, Harper JW. Cell cycle-regulated phosphorylation of p220(NPAT) by cyclin E/Cdk2 in Cajal bodies promotes histone gene transcription. *Genes & development* 2000; 14:2298-313; PMID:10995387; <http://dx.doi.org/10.1101/gad.829500>
- [43] Gao G, Bracken AP, Burkard K, Pasini D, Classon M, Attwooll C, Sagara M, Imai T, Helin K, Zhao J. NPAT expression is regulated by E2F and is essential for cell cycle progression. *Mol Cell Biol* 2003; 23:2821-33; PMID:12665581; <http://dx.doi.org/10.1128/MCB.23.8.2821-2833.2003>
- [44] Yang XC, Sabath I, Kunduru L, van Wijnen AJ, Marzluff WF, Dominski Z. A conserved interaction that is essential for the biogenesis of histone locus bodies. *J Biol Chem* 2014; 289:33767-82; PMID:25339177; <http://dx.doi.org/10.1074/jbc.M114.616466>
- [45] Tuupanen S, Turunen M, Lehtonen R, Hallikas O, Vanharanta S, Kivioja T, Bjorklund M, Wei G, Yan J, Niittymaki I, et al. The common colorectal cancer predisposition SNP rs6983267 at chromosome 8q24 confers potential to enhanced Wnt signaling. *Nat Genet* 2009; 41:885-90; PMID:19561604; <http://dx.doi.org/10.1038/ng.406>
- [46] Wei GH, Badis G, Berger MF, Kivioja T, Palin K, Enge M, Bonke M, Jolma A, Varjosalo M, Gehrke AR, et al. Genome-wide analysis of ETS-family DNA-binding in vitro and in vivo. *EMBO J* 2010; 29:2147-60; PMID:20517297; <http://dx.doi.org/10.1038/emboj.2010.106>
- [47] Van der Laan MJ, Pollard KS. A new algorithm for hybrid hierarchical clustering with visualization and the bootstrap. *J Statistical Planning Inference* 2003; 117:275-303; [http://dx.doi.org/10.1016/S0378-3758\(02\)00388-9](http://dx.doi.org/10.1016/S0378-3758(02)00388-9)
- [48] Gautier L, Cope L, Bolstad BM, Irizarry RA. affy—analysis of Affymetrix GeneChip data at the probe level. *Bioinformatics* 2004; 20:307-15; PMID:14960456; <http://dx.doi.org/10.1093/bioinformatics/btg405>
- [49] Smyth GK. Linear models and empirical bayes methods for assessing differential expression in microarray experiments. *Statistical applications in genetics and molecular biology* 2004; 3: Article3; PMID:16646809; <http://dx.doi.org/10.2202/1544-6115.1027>
- [50] Dai M, Wang P, Boyd AD, Kostov G, Athey B, Jones EG, Bunney WE, Myers RM, Speed TP, Akil H, et al. Evolving gene/transcript definitions significantly alter the interpretation of GeneChip data. *Nucleic Acids Res* 2005; 33:e175; PMID:16284200; <http://dx.doi.org/10.1093/nar/gni179>
- [51] Mali P, Yang L, Esvelt KM, Aach J, Guell M, DiCarlo JE, Norville JE, Church GM. RNA-guided human genome engineering via Cas9. *Science* 2013; 339:823-6; PMID:23287722; <http://dx.doi.org/10.1126/science.1232033>
- [52] Henry-Mowatt J, Jackson D, Masson JY, Johnson PA, Clements PM, Benson FE, Thompson LH, Takeda S, West SC, Caldecott KW. XRCC3 and Rad51 modulate replication fork progression on damaged vertebrate chromosomes. *Mol Cell* 2003; 11:1109-17; PMID:12718895; [http://dx.doi.org/10.1016/S1097-2765\(03\)00132-1](http://dx.doi.org/10.1016/S1097-2765(03)00132-1)